5146 *J. Phys. Chem. A* **2001,** *105,* 5146−5154

Atmospheric Oxidation Mechanism of Methyl Formate

T. J. Wallington* and M. D. Hurley
Ford Research Laboratory, SRL-3083, Ford Motor Company, P.O. Box 2053, Dearborn, Michigan 48121-2053

T. Maurer, I. Barnes, and K. H. Becker
Bergische Universität GH Wuppertal / FB 9 - Physikalische Chemie, Gaussstrasse 20,
D-42097 Wuppertal, Germany

G. S. Tyndall and J. J. Orlando
Atmospheric Chemistry Division, National Center for Atmospheric Research, Boulder, Colorado 80305

A. S. Pimentel
Departamento de Físico-Química, Instituto de Química, Universidade Federal do Rio de Janeiro,
21949-900 Rio de Janeiro, Brazil

M. Bilde
Department of Chemistry, University of Copenhagen, Universitetsparken 5, 2100 Copenhagen Ø, Denmark

Received: November 9, 2000; In Final Form: March 14, 2001

The products following Cl atom initiated oxidation of methyl formate in 700−760 Torr of air in the presence and absence of NO_x at 296 ± 2 K were investigated using three different FTIR smog chamber techniques. Reaction of Cl atoms with methyl formate proceeds 45 ± 7% via attack at the methyl group (forming $HC(O)OCH_2\cdot$ radicals) and 55 ± 7% via attack at the formate group (forming $\cdot C(O)OCH_3$ radicals). The sole atmospheric fate of $HC(O)OCH_2\cdot$ and $\cdot C(O)OCH_3$ radicals is addition of O_2 to give the corresponding peroxy radicals ($HC(O)OCH_2OO\cdot$ and $\cdot OOC(O)OCH_3$). The peroxy radicals react with NO to give alkoxy radicals ($HC(O)OCH_2O\cdot$ and $\cdot OC(O)OCH_3$). The atmospheric fate of $\cdot OC(O)OCH_3$ radicals is decomposition to give $CH_3O\cdot$ and CO_2 and was unaffected by the method used to generate the $\cdot OC(O)OCH_3$ radicals (reaction of $\cdot OOC(O)OCH_3$ with either NO or with other peroxy radicals). There are two competing atmospheric loss mechanisms for $HC(O)OCH_2O\cdot$ radicals; reaction with O_2 to give $HC(O)OC(O)H$ (formic acid anhydride) and α-ester rearrangement to give $HC(O)OH$ and $HCO\cdot$ radicals. It was found that α-ester rearrangement is more important when $HC(O)OCH_2O\cdot$ radicals were produced via the $HC(O)OCH_2OO\cdot + NO$ reaction than when they were produced via the self-reaction of peroxy radicals. We ascribe this observation to the formation of vibrationally excited $HC(O)OCH_2O\cdot$ radicals in the $HC(O)OCH_2OO\cdot + NO$ reaction. In 1 atm of air ($[O_2] = 160$ Torr) containing NO at 296 K, it can be calculated that 33 ± 5% of the $HC(O)OCH_2O\cdot$ radicals undergo α-ester rearrangement, while 67 ± 12% react with O_2. The infrared spectrum of the peroxynitrate $CH_3OC(O)OONO_2$ was recorded, and absorption cross sections (base e) of $(1.8 \pm 0.1) \times 10^{-18}$ and $(4.2 \pm 0.2) \times 10^{-18}$ cm^2 molecule^{-1} at 1836 and 1236 cm^{-1}, respectively, were determined. The chain chlorination of methyl formate was studied. Relative rate techniques were used to measure $k(Cl + ClC(O)OCH_3) = (1.10 \pm 0.23) \times 10^{-13}$, $k(Cl + HC(O)OCH_2Cl) = (2.5 \pm 0.2) \times 10^{-13}$, and $k(Cl + ClC(O)OCH_2Cl) = (3.0 \pm 0.4) \times 10^{-14}$ cm^3 molecule^{-1} s^{-1}. IR spectra of $ClC(O)OCH_2Cl$, $ClC(O)OCHCl_2$, and $ClC(O)OCCl_3$ are presented. These results are discussed with respect to the atmospheric oxidation mechanism of methyl formate and other esters.

1. Introduction

Esters are used as reagents during the manufacture of perfumes and food flavoring and are employed as industrial solvents. Prompted by the need for more environmentally compatible solvents, (i.e., compounds which will reduce the level of photooxidant formation in the troposphere), there is commercial interest in the use of esters as replacements for traditional solvents. Esters are volatile organic compounds and may be released into the atmosphere during their use (methyl formate has a boiling point of 34 °C). Esters are also emitted into the atmosphere from natural sources (i.e., vegetation) and are formed in the atmosphere as oxidation products of ethers used as automotive fuel additives.[1−4] Increased use of esters as solvents will lead to increased emissions into the atmosphere. Assessment of the contribution of esters to photooxidant formation in urban air masses requires detailed kinetic and mechanistic information concerning their atmospheric oxidation.

The atmospheric oxidation mechanism of esters has received relatively little attention, and its representation in atmospheric models has substantial uncertainty. To improve our understand-

---

* Corresponding author. E-mail: twalling@ford.com.

10.1021/jp0041398 CCC: $20.00

ing of the atmospheric chemistry of esters and to facilitate an accurate description of such in atmospheric models, we have conducted a study of the atmospheric oxidation mechanism of methyl formate. Methyl formate is the simplest ester, and a study of its chemistry provides useful insight into the atmospheric oxidation mechanism of this class of organic compounds.

The atmospheric oxidation of methyl formate is initiated by reaction with OH radicals

$$OH + HC(O)OCH_3 \rightarrow \cdot C(O)OCH_3 + H_2O \qquad (1a)$$

$$OH + HC(O)OCH_3 \rightarrow HC(O)OCH_2\cdot + H_2O \qquad (1b)$$

Under atmospheric conditions, alkyl radicals produced in reaction 1 react with oxygen to give peroxy radicals

$$\cdot C(O)OCH_3 + O_2 + M \rightarrow \cdot OOC(O)OCH_3 + M \qquad (2)$$

$$HC(O)OCH_2\cdot + O_2 + M \rightarrow HC(O)OCH_2OO\cdot + M \qquad (3)$$

Peroxy radicals react with NO, NO_2, HO_2, and other peroxy radicals in the atmosphere.[5,6] Reaction with NO dominates in polluted air masses and proceeds via two channels giving alkoxy radicals as major and organic nitrates as minor products.[5] In this work, we have studied the atmospheric fate of $\cdot OOC(O)OCH_3$ and $HC(O)OCH_2OO\cdot$ radicals. The alkoxy radicals were prepared by UV irradiation of methyl formate/Cl_2/N_2/O_2 mixtures in the presence and absence of NO in 700−760 Torr total pressure of N_2/O_2 diluent at 296 ± 2 K. As part of this work, the mechanism of the reaction of Cl atoms with methyl formate, the kinetics of the reactions of Cl atoms with $ClC(O)OCH_3$, $HC(O)OCH_2Cl$, and $ClC(O)OCH_2Cl$, and the IR spectra of $ClC(O)OCH_2Cl$, $ClC(O)OCHCl_2$, and $ClC(O)OCCl_3$ were determined.

2. Experimental Section

Experiments were performed using the photoreactors at Ford,[7] Bergische Universität GH Wuppertal,[8] and the National Center for Atmospheric Research (NCAR).[9] The experimental systems are described in detail elsewhere and are discussed briefly here. In all three laboratories, the degradation of methyl formate was initiated by reaction with Cl atoms generated by the photolysis of molecular chlorine in N_2/O_2 diluent, with products determined by in situ FTIR spectroscopy

$$Cl_2 + h\nu \rightarrow 2\,Cl \qquad (4)$$

$$Cl + HC(O)OCH_3 \rightarrow HCl + \cdot C(O)OCH_3 \qquad (5a)$$

$$Cl + HC(O)OCH_3 \rightarrow HCl + HC(O)OCH_2\cdot \qquad (5b)$$

2.1. FTIR−Smog Chamber System at Ford Motor Company.

Experiments were performed in a 140 L Pyrex reactor interfaced to a Mattson Sirus 100 FTIR spectrometer. The reactor was surrounded by 22 fluorescent blacklamps (GE F15T8-BL), which were used to photochemically initiate the experiments. Loss of methyl formate and formation of products were monitored by Fourier transform infrared spectroscopy using an infrared path length of 27.4 m and a resolution of 0.25 cm^{-1}. Infrared spectra were derived from 32 co-added interferograms which took 90 s to acquire, co-add, and transform.

The mechanism of the reaction of Cl atoms with methyl formate was investigated by irradiating methyl formate/Cl_2 mixtures in 700 Torr total pressure of N_2 diluent at 296 ± 2 K. Initial concentrations of the gas mixtures were (2−5) × 10^{14} and (1−5) × 10^{15} molecule cm^{-3} for methyl formate and Cl_2. Reagents were obtained from commercial sources at the following purities: methyl formate (>99%), Cl_2 (>99.8%), NO (>99.95%), N_2 (>99.995%), O_2 (>99.995%), and synthetic air (>99.995%).

In smog chamber experiments, unwanted losses of reactants and products via photolysis, dark chemistry, and wall reactions have to be considered. Each experiment lasted 15−25 min, with total photolysis times not exceeding 7 min (4−7 irradiations). Control experiments were performed to check for unwanted losses in the chamber. No significant loss (<2%) of formic acid, formic acid anhydride, CO, or CO_2 was observed when mixtures of these compounds in air were irradiated for 10 min or left in the dark for 20 min, showing that photolytic and heterogeneous losses of these compounds in the chamber are not important.

2.2. FTIR System at the National Center for Atmospheric Research (NCAR).

Experiments were conducted in a 47 L stainless steel chamber using a Bomem DA3.01 FTIR spectrometer for analysis. The oxidation of methyl formate was initiated using Cl atoms formed via photolysis of Cl_2 using a filtered xenon arc lamp. Reactant loss and product formation were monitored by FTIR absorption spectroscopy, using an optical path length of 32.6 m and a spectral resolution of 1.0 cm^{-1}. Infrared spectra were derived from 200 co-added interferograms (acquistion time = 4 min). Typical photolysis times were 4−5 min.

Three sets of experiments were performed at NCAR. First, UV irradiation of Cl_2/$HC(O)OCH_3$/N_2/O_2 mixtures with differing partial pressures of O_2 (10−350 Torr) was employed to determine the position of Cl atom attack. Second, UV irradiation of Cl_2/$HC(O)OCH_3$/NO_2/N_2/O_2 mixtures was used to determine the IR absorption cross sections of $CH_3OC(O)O_2NO_2$. Third, UV irradiation of Cl_2/$HC(O)OCH_3$/NO/N_2/O_2 mixtures was employed to study the product yields in the presence of NO. The methyl formate concentration was typically 3.5 × 10^{14} (for experiments conducted in absence of NO_x) or 8.8 × 10^{14} (for experiments conducted in the presence of NO_x), while those of NO and NO_2 were approximately 6 × 10^{14} and 3.5 × 10^{14} molecule cm^{-3}, respectively. CO and CO_2 were quantified using reference spectra calibrated by expanding known amounts of the pure compounds into the chamber. Formic acid anhydride (FAA), HC(O)OC(O)H, was quantified using a calibrated spectrum from the IR library at Ford ($\sigma = 1.67 \times 10^{-18}$ and 5.72×10^{-19} cm^2 $molecule^{-1}$ (base e) at 1775 and 1829 cm^{-1}), which was in excellent agreement (within 5%) with the spectrum acquired at Wuppertal. Reagents were obtained from commercial sources at the following purities: methyl formate (>99%), Cl_2 (>99.5%), NO (>98.5%), nitrogen (>99.995%), oxygen (>99.995%) and synthetic air (>99.995%). NO_2 was prepared from NO by reaction with excess O_2 followed by distillation at 196 K. Neither the NO or the NO_2 contained more than 1% impurity identifiable in the IR spectra.

2.3. FTIR−Photoreactor System at Bergische Universität GH Wuppertal.

Experiments were carried out in a 1080 L quartz-glass photoreactor equipped with a built-in White mirror system. The photolysis of chlorine (Cl_2) with fluorescent lamps (Philips Tl 40W/05, 320 < λ < 450 nm) was used to generate Cl atoms. Concentrations of reactants were monitored by long path in situ FTIR spectroscopy. The FTIR spectrometer (Bruker IFS-88) was operated with a resolution of 1 cm^{-1} using a path length of 484.7 m. All experiments were carried out at 1000 mbar total pressure in synthetic air or mixtures of (N_2 + O_2) at 298 ± 2 K. During irradiation, between 10 and 20 min, 10 spectra with 60/120 scans (1/2 min) were collected. Typical initial concentrations were 10 ppm for Cl_2, 0.6−0.7 ppm for

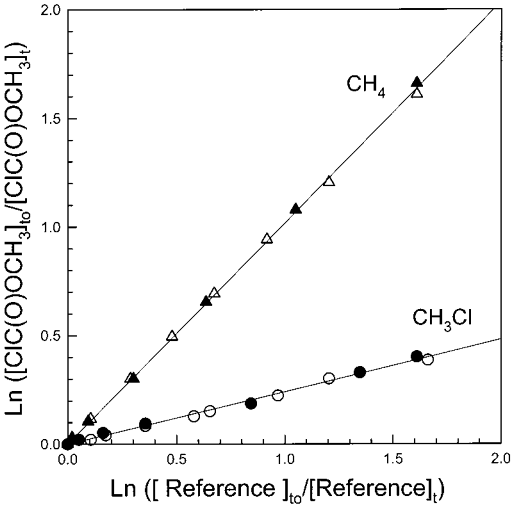

Figure 1. Loss of $ClC(O)OCH_3$ vs reference compounds CH_4 and CH_3Cl following exposure to Cl atoms in 700 Torr of air (filled symbols) or N_2 (open symbols) at 296 K.

methyl formate, and 3−4 ppm for NO (1 ppm = 2.46×10^{13} molecule cm^{-3} at 1000 mbar and 298 K). Reagents were obtained from commercial sources at the following purities: methyl formate (>99%), Cl_2 (>99.8%), NO (>99.95%), NO_2 (>99.95%), nitrogen (>99.995%), oxygen (>99.995%), and synthetic air (>99.995%).

3 Results

3.1. Relative Rate Study of *k*(Cl + ClC(O)OCH$_3$) at Ford. To aid investigation of the mechanism of the reaction of Cl atoms with methyl formate, we first performed relative rate experiments to study the kinetics of reactions of Cl with methyl chloroformate ($ClC(O)OCH_3$). Reaction 6 was studied relative to reactions 7 and 8

$$Cl + ClC(O)OCH_3 \rightarrow \text{products} \tag{6}$$

$$Cl + CH_4 \rightarrow \text{products} \tag{7}$$

$$Cl + CH_3Cl \rightarrow \text{products} \tag{8}$$

Figure 1 shows plots of the loss of $ClC(O)OCH_3$ versus CH_4 and CH_3Cl following exposure to Cl atoms in 700 Torr of either air (filled symbols) or N_2 (open symbols) at 296 K. There was no discernible difference between data obtained in air or N_2 diluent. Linear least-squares analysis of the data in Figure 1 gives rate constant ratios $k_6/k_7 = 1.02 \pm 0.10$ and $k_6/k_8 = 0.241 \pm 0.031$ (quoted errors are two standard deviations). The relative rate data can be placed upon an absolute basis using $k_7 = 1.0 \times 10^{-13}$ [10] and $k_8 = 4.9 \times 10^{-13}$ [10] to give $k_6 = (1.02 \pm 0.10) \times 10^{-13}$ and $(1.18 \pm 0.15) \times 10^{-13}$ cm^3 $molecule^{-1}$ s^{-1}. The values of k_6 obtained using the two different reference compounds were indistinguishable within the experimental uncertainties, suggesting the absence of substantial systematic errors associated with the use of individual reference reactions. We choose to quote a final value of k_6 which is the average of the individual measurements, together with error limits which encompass the extremes of the individual determinations. Hence, $k_6 = (1.10 \pm 0.23) \times 10^{-13}$ cm^3 $molecule^{-1}$ s^{-1}. We estimate that potential systematic errors associated with uncertainties in the reference rate constants contribute an additional 10% to the uncertainty range. There are no previous studies of this reaction to compare with our results.

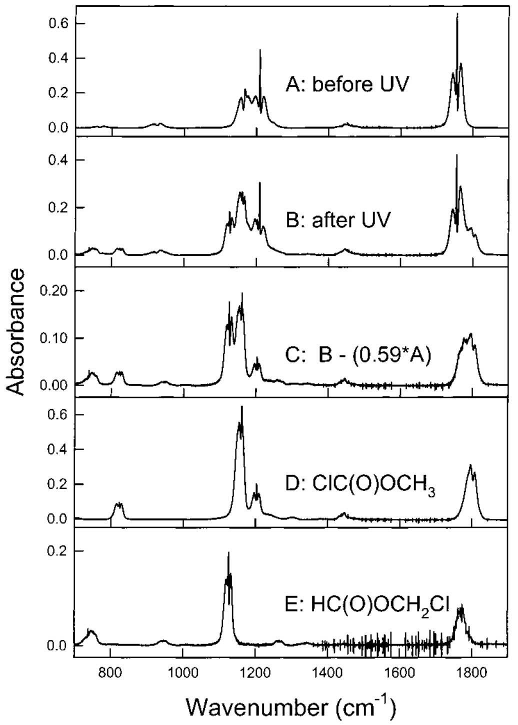

Figure 2. Spectra acquired before (A) and after (B) a 3 s irradiation of a mixture containing 7.4 mTorr methyl formate and 102 mTorr of Cl_2 in 700 Torr of N_2. Subtraction of features attributable to methyl formate from panel B gives the product spectrum given in panel C. Panel D is a reference spectrum of $ClC(O)OCH_3$. Subtraction of $ClC(O)OCH_3$ features from panel D gives panel E, which is assigned to $HC(O)OCH_2Cl$.

3.2. Mechanistic Study of the Reaction of Cl Atoms with HC(O)OCH$_3$ at Ford. To ascertain the relative importance of Cl atom attack at the CH_3- and HC(O)-ends of the methyl formate molecule, we performed experiments in which mixtures of $HC(O)OCH_3$ and Cl_2 in 760 Torr of N_2 diluent were subjected to UV irradiation. The alkyl radicals formed following H atom abstraction react with Cl_2 to give either $HC(O)OCH_2Cl$ or $ClC(O)OCH_3$

$$HC(O)OCH_3 + Cl \rightarrow {\cdot}C(O)OCH_3 + HCl \tag{5a}$$

$$HC(O)OCH_3 + Cl \rightarrow HC(O)OCH_2{\cdot} + HCl \tag{5b}$$

$$HC(O)OCH_2{\cdot} + Cl_2 \rightarrow HC(O)OCH_2Cl + Cl \tag{9a}$$

$${\cdot}C(O)OCH_3 + Cl_2 \rightarrow ClC(O)OCH_3 + Cl \tag{9b}$$

The yields of $ClC(O)OCH_3$ and $HC(O)OCH_2Cl$ provide information on the branching ratio k_{5a}/k_{5b}. Fortunately, high-purity (>99%) $ClC(O)OCH_3$ is commercially available allowing calibration of the FTIR spectrometer system. Figure 2 shows IR spectra acquired before (A) and after (B) a 3 s irradiation of a mixture of 7.4 mTorr of $HC(O)OCH_3$ and 102 mTorr of Cl_2 in 700 Torr of N_2 diluent (1 mTorr = 3.2×10^{13} molecule cm^{-3}). Subtraction of IR features attributable to $HC(O)OCH_3$ from panel B gives the product spectrum shown in panel C. Comparison with a reference spectrum of $ClC(O)OCH_3$ given in panel D shows the formation of this species. Subtraction of IR features attributed to $ClC(O)OCH_3$ from panel C gives the residual spectrum in panel E, which we assign to $HC(O)OCH_2Cl$.

Figure 3 shows a plot of the observed formation of $ClC(O)OCH_3$ versus loss of $HC(O)OCH_3$ following the UV irradiation

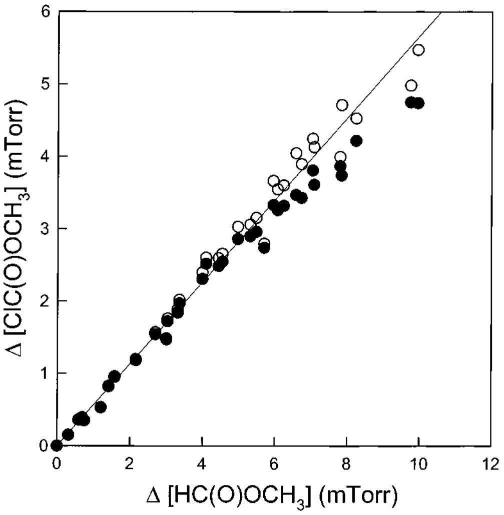

Figure 3. Formation of ClC(O)OCH$_3$ vs loss of methyl formate following UV irradiation of methyl formate/Cl$_2$/N$_2$ mixtures. Filled symbols are observed data; open symbols have been corrected for secondary reaction with Cl atoms (see text for details).

of HC(O)OCH$_3$/Cl$_2$/N$_2$ mixtures. As with all product studies, it is important to consider and, where necessary, correct for the loss of products via secondary reactions in the system. To test for loss of HC(O)OCH$_2$Cl and ClC(O)OCH$_3$ via heterogeneous processes, we allowed reaction mixtures to stand in the dark in the chamber for 30 min. No loss ($<2\%$) of either HC(O)OCH$_2$Cl or ClC(O)OCH$_3$ was observed, indicating the absence of unwanted heterogeneous reactions. As discussed in the previous section, Cl atoms react with ClC(O)OCH$_3$ with a rate constant of $k_6 = (1.10 \pm 0.23) \times 10^{-13}$ cm^3 molecule^{-1} s^{-1}. Corrections for loss via reaction 6 can be computed using the expression[14]

$$\text{correction factor} = \left[\frac{x}{\left(\dfrac{1}{1-\dfrac{k_6}{k_5}}\right)((1-x)[(1-x)^{\{(k_6/k_5)-1\}}-1])}\right]$$

The "correction factor" is the factor by which the observed ClC(O)OCH$_3$ yield needs to be multiplied to account for secondary loss via reaction 6, "x" is the fractional consumption of methyl formate, and k_6 and k_5 are the bimolecular rate constants for reaction of Cl atoms with ClC(O)OCH$_3$ and HC(O)OCH$_3$. Reaction of Cl atoms with ClC(O)OCH$_3$ is 1.4×10^{-12} [11]/$1.10 \times 10^{-13} = 13$ times slower than that with HC(O)OCH$_3$, and the corrections are modest. The open symbols in Figure 3 show the result of correcting the measured ClC(O)OCH$_3$ data (filled symbols) for secondary loss via reaction 6.

Linear least-squares analysis of the corrected data in Figure 3 gives a molar yield of ClC(O)OCH$_3$ of 0.55 ± 0.05 (the uncertainty is 2 standard deviations, obtained from the linear least-squares analysis). We estimate that the absolute calibrations of the reference spectra of HC(O)OCH$_3$ and ClC(O)OCH$_3$ each have a 5% uncertainty. Propagation of these uncertainties gives a final molar yield of ClC(O)OCH$_3$ of 0.55 ± 0.07. We conclude that $k_{5a}/(k_{5a} + k_{5b}) = 0.55 \pm 0.07$ and, by inference, $k_{5b}/(k_{5a} + k_{5b}) = 0.45 \pm 0.07$. This result can be compared to the findings from a recent computational study by Good et al.[12] In the abstract of their paper, Good et al.[12] report that "it is found that 90% of the reaction proceeds via abstraction of the carbonyl hydrogen" (i.e., $k_{5a}/(k_{5a} + k_{5b}) = 0.90$). However, in the body of their paper, Good et al.[12] state that taking reasonable estimates of the uncertainties associated with computed activation energies $k_{5a}/(k_{5a} + k_{5b})$ could range from 0.65 to 0.97. The experimental results reported herein are clearly inconsistent with $k_{5a}/(k_{5a} + k_{5b}) = 0.90$ and are also significantly lower than the lowest extreme of the range of $k_{5a}/(k_{5a} + k_{5b}) = 0.65-0.90$ reported in the computational study of Good et al.[12] Finally, we note that our measurement of $k_{5a}/(k_{5a} + k_{5b}) = 0.55 \pm 0.07$ is inconsistent with the prediction of $k_{5a}/(k_{5a} + k_{5b}) \approx 0$ from the structure activity relationship derived by Notario et al.[13]

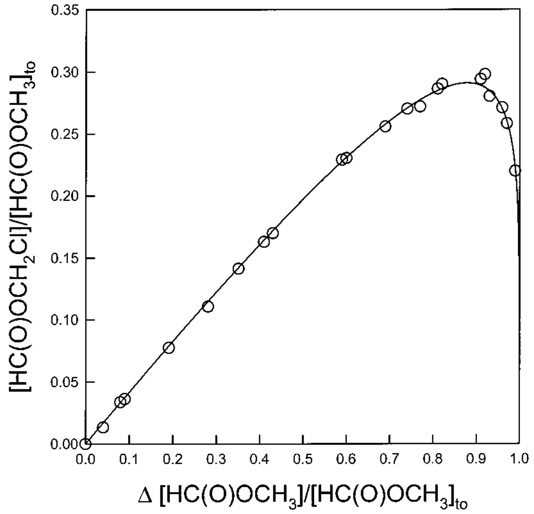

Figure 4. Plot of the observed concentration of HC(O)OCH$_2$Cl normalized to the initial methyl formate concentration vs the fractional loss of methyl formate following irradiation of mixtures of methyl formate and Cl$_2$ in 700 Torr of air diluent. The curve is a fit to the data; see text for details.

The infrared product features in Figure 2E assigned to HC(O)OCH$_2$Cl increased in intensity as HC(O)OCH$_3$/Cl$_2$/N$_2$ mixtures were subjected to successive UV irradiation. To obtain a calibrated HC(O)OCH$_2$Cl spectrum, it was assumed that in experiments with low conversions ($<20\%$) of HC(O)OCH$_3$, the spectral features remaining after subtraction of HC(O)OCH$_3$ and ClC(O)OCH$_3$ are attributable entirely to HC(O)OCH$_2$Cl. For HC(O)OCH$_3$ consumptions $>80\%$, the yield of HC(O)OCH$_2$Cl reached a plateau, and for consumptions $>90\%$, the HC(O)OCH$_2$Cl yield decreased. We ascribe this behavior to loss of HC(O)OCH$_2$Cl via secondary reaction with Cl atoms

$$\text{HC(O)OCH}_2\text{Cl} + \text{Cl} \rightarrow \text{products} \qquad (10)$$

Figure 4 shows a plot of the fraction of the initial HC(O)OCH$_3$ converted into HC(O)OCH$_2$Cl versus the fractional consumption of HC(O)OCH$_3$. The appropriate rate equations can be solved analytically[14] to relate the amount of HC(O)OCH$_2$Cl at any time t to the corresponding conversion of HC(O)OCH$_3$ as a function of $k_{5b}/(k_{5a} + k_{5b})$, defined below as "α", and the rate constant ratio k_{10}/k_5 where k_{10} and k_5 are the bimolecular rate constants of reactions 10 and 5, respectively. The expression is[14]

$$\frac{[\text{HC(O)OCH}_2\text{Cl}]_t}{[\text{HC(O)OCH}_3]_{t_0}} = \frac{\alpha}{1-\dfrac{k_{10}}{k_5}}(1-x)[(1-x)^{\{(k_{10}/k_5)-1\}}-1] \qquad (\text{I})$$

where x is the conversion of HC(O)OCH$_3$, defined as

$$x \equiv 1 - \frac{[\text{HC(O)OCH}_3]_t}{[\text{HC(O)OCH}_3]_{t_0}}$$

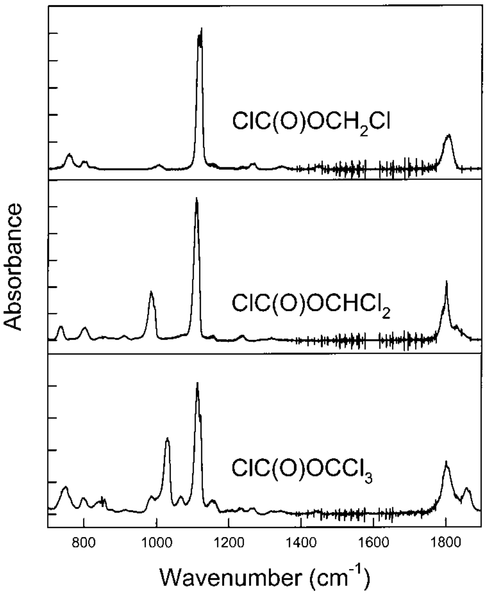

Figure 5. IR spectra of $ClC(O)OCH_2Cl$, $ClC(O)OCHCl_2$, and $ClC(O)OCCl_3$.

A fit of expression I to the data in Figure 4 gives $k_{5b}/(k_{5a} + k_{5b}) = 0.42 \pm 0.04$ and $k_{10}/k_5 = 0.177 \pm 0.015$. Using $k_5 = 1.4 \times 10^{-12}$ gives $k_{10} = (2.5 \pm 0.2) \times 10^{-13}$ cm^3 molecule^{-1} s^{-1}.

For completeness, experiments were conducted using mixtures of 6−8 mTorr of $ClC(O)OCH_3$ and 100 mTorr of Cl_2 in 700 Torr of N_2 diluent to study the chain chlorination of $ClC(O)OCH_3$. Following successive periods of 1−10 s of UV irradiation, the IR features attributable to $ClC(O)OCH_3$ decreased and were replaced by IR features of an unknown product(s) at 757, 800, 1116, 1264, and 1806 cm^{-1}, which we will designate “X”. Further irradiation of the sample led to increases of the IR features of the unknown(s) until the consumption of $ClC(O)OCH_3$ was almost complete (>85% loss). Continued irradiation led to little or no increase in X until all the $ClC(O)OCH_3$ had been consumed (>95%), at which point the concentration of X started to decrease. The IR features attributed to “X” scaled linearly with each other during both formation and loss in the chamber, suggesting (but not proving) that they are all attributable to a single chemical species. To test for reactions occurring in the absence of UV light, we allowed reaction mixtures to stand in the dark for 10 min between irradiations; there was no observable change in the IR spectra, showing the absence of complications associated with “dark chemistry”. The fact that little or no loss of X was observed until almost all of the $ClC(O)OCH_3$ had been consumed shows that its reactivity toward Cl atoms is substantially less than that of $ClC(O)OCH_3$. Further irradiation led to a decrease in X and the formation of a new set of unknown IR features at 736, 800, 984, 1109, and 1802 cm^{-1}. This second set of IR product features increased at the expense of X upon further irradiation. Only when >80% of X was consumed did the second set of unknown features decrease. The IR features of the second unknown scaled linearly during both formation and loss in the chamber, again suggesting (but not proving) that they are all attributable to a single chemical species which we will designate “Y”. Y is much less reactive toward Cl atoms than X. Finally, continued irradiation lead to the decrease in “Y” and the formation of another set of IR features at 749, 1029, 1114, 1803, and 1858 cm^{-1}, which we assign to compound “Z” and which do not decrease upon continued UV irradiation. The simplest interpretation of the observations is to assign X, Y, and Z to $ClC(O)OCH_2Cl$, $ClC(O)OCHCl_2$, and $ClC(O)OCCl_3$, respectively. The IR spectra for these species are given in Figure 5. From the formation and subsequent loss of $ClC(O)OCH_2Cl$, a rate constant ratio of $k_{11}/k_6 = 0.269 \pm 0.023$ was established, which, when combined with $k_6 = (1.10 \pm 0.12) \times 10^{-13}$, gives $k_{11} = (3.0 \pm 0.4) \times 10^{-14}$ cm^3 molecule^{-1} s^{-1}

$$Cl + ClC(O)OCH_2Cl \rightarrow \text{products} \qquad (11)$$

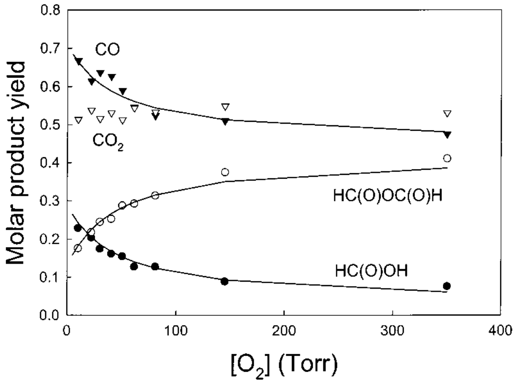

Figure 6. Yields of CO_2 (open triangles), CO (filled triangles), formic acid anhydride (open circles), and HC(O)OH (filled circles) observed following the UV irradiation of $HC(O)OCH_3/Cl_2/O_2/N_2$ mixtures at 296 K at 700 Torr total pressure of N_2/O_2 diluent vs O_2 partial pressure. The curves are fits to the data; see text for details.

3.3. Products of Cl Initiated Oxidation of Methyl Formate in N_2/O_2 Mixtures at NCAR. As a preliminary exercise, experiments were performed using the UV irradiation of $HC(O)OCH_3/Cl_2/N_2$ mixtures (i.e., in the absence of O_2) in the experimental system at NCAR to double check the results presented above. IR product features attributable to both $ClC(O)OCH_3$ and $HC(O)OCH_2Cl$ were detected, with relative peak heights which were indistinguishable from those observed in the experiments described in the previous section. There was no observable HCHO, CO, or CO_2 (molar yields <5%) produced as a result of the UV photolysis of $HC(O)OCH_3/Cl_2/N_2$ mixtures, showing that the decomposition of the $\cdot C(O)OCH_3$ and $HC(O)OCH_2\cdot$ radicals produced in reaction 5 is not competitive with their reaction with Cl_2.

To investigate the products of the Cl atom initiated oxidation of methyl formate, we performed experiments in which $HC(O)OCH_3/Cl_2/N_2/O_2$ mixtures were exposed to five successive UV irradiations (each of 4 min duration). IR spectra were acquired after each period of irradiation. Experiments were performed at a total pressure of 700 Torr, with the O_2 partial pressure varied over the range of 10−350 Torr. The following carbon containing products were identified: CO, CO_2, HC(O)OH, and HC(O)OC(O)H (formic acid anhydride). Plots of the formation of the products versus loss of methyl formate were linear and were used to derive molar product yields. Figure 6 shows a plot of the molar product yields of HC(O)OH, HC(O)OC(O)H, CO, and CO_2 versus the O_2 partial pressure. Within the experimental uncertainties, the combined yields of HC(O)OH, HC(O)OC(O)H, CO, and CO_2 account for 90−100% of the loss of methyl formate. After subtraction of absorption features due to the above compounds, an absorption always remained at 1308 cm^{-1}, which is close to that of dimethyl carbonate, $CH_3OC(O)OCH_3$.[15] This absorption was assigned an absorption cross section (base e) of 2×10^{-18} cm^2 molecules^{-1} by analogy to dimethyl carbonate.[15] Since it is independent of O_2 (yield 10%), it is probably formed from the $\cdot C(O)CH_3$ radical and may be an acid or peracid (or both) formed in a reaction of the peroxyacyl radical, e.g.

$$\cdot OOC(O)OCH_3 + HO_2 \rightarrow HOOC(O)OCH_3 + O_2 \text{ or } HOC(O)OCH_3 + O_3 \quad (12)$$

As seen from Figure 6, the yield of CO_2 was 50−55%, independent of $[O_2]$. The yield of formic acid anhydride increased with increasing $[O_2]$ over the range 10−350 Torr, while those of CO and HC(O)OH decreased with increasing $[O_2]$. The observation that the yield of formic acid anhydride increases with increasing O_2 partial pressure while that of formic acid decreases with increasing O_2 partial pressure suggests that reaction with O_2 to give formic acid anhydride and decomposition to formic acid and a formyl (HCO) radical are competing fates of the $HC(O)OCH_2O\cdot$ radical

$$HC(O)OCH_2O\cdot + O_2 \rightarrow HO_2 + HC(O)OC(O)H \quad (13)$$

$$HC(O)OCH_2O\cdot + M \rightarrow HCO + HC(O)OH + M \quad (14)$$

$$HCO + O_2 \rightarrow HO_2 + CO \quad (15)$$

Reaction 14 is the α-ester rearrangement first observed by Tuazon et al.,[16] in which an alkoxy radical $RC(O)OCH(O\cdot)R'$ undergoes rapid rearrangement and decomposition to RC(O)OH and $R'C(\cdot)O$ via a five-membered ring transition state. The α-ester rearrangement has been observed in the oxidation of methyl acetate,[17] ethyl acetate,[16] methyl propionate,[18] ethylene glycol diformate,[19] and $CF_3C(O)OCH_2CF_3$ [20] and appears to be a general feature in the atmospheric oxidation mechanism of esters.

Abstraction of H from the HC(O) group is expected to lead to the formation of CO_2 and HCHO, which will be rapidly converted to CO in the presence of Cl atoms; thus, the CO yield contains components that are both dependent on, and independent of, O_2. The high-O_2 limiting values for CO and CO_2 provide a measure of the importance of attack of Cl atoms at the HC(O) group in methyl formate.[12] As seen from Figure 6, the high-O_2 limiting values for CO and CO_2 are consistent with the branching ratio $k_{5a}/(k_{5a} + k_{5b}) = 0.55 \pm 0.07$ derived in section 3.2. Similarly, the sum of the HC(O)OH and HC(O)OC(O)H (formic acid anhydride) yields provides a measure of the Cl atom attack on the methyl group in methyl formate and is consistent with the branching ratio $k_{5b}/(k_{5a} + k_{5b}) = 0.45 \pm 0.07$ derived in section 3.2. It should be noted that Good et al.[12] also observed substantial yields of FAA and HC(O)OH in their experimental study but did not quantify them.

Assuming that reactions 13 and 14 are the sole fate of $HC(O)OCH_2O\cdot$ radicals, the dependence of the HC(O)OC(O)H, HC(O)OH and CO yields on $[O_2]$ can be expressed in terms of the rate constant ratio k_{13}/k_{14}. The yield of HC(O)OC(O)H is given by

$$Y(HC(O)OC(O)H) = Y(RO\cdot)\left(\frac{\frac{k_{13}}{k_{14}}[O_2]}{\frac{k_{13}}{k_{14}}[O_2] + 1}\right) + C \quad (II)$$

where $Y(RO\cdot)$ is the yield of the $HC(O)OCH_2O\cdot$ radical. The term C in eq II accounts for formation of HC(O)OC(O)H via channels that are independent of O_2 concentration, e.g., via the molecular channel of the $HC(O)OCH_2OO\cdot$ peroxy radical self-reaction. The yields of HC(O)OH and CO have the same functional dependence. For HC(O)OH

$$Y(HC(O)OH) = Y(RO\cdot)\left(\frac{1}{\frac{k_{13}}{k_{14}}[O_2] + 1}\right) + C' \quad (III)$$

where C' represents the yield of HC(O)OH via processes which are independent of O_2. The curves through the HC(O)OC(O)H, HC(O)OH, and CO data in Figure 6 are simultaneous least-squares fits of expressions II and III to the data which gives $k_{13}/k_{14} = 0.022 \pm 0.004$ Torr^{-1}. As seen from Figure 6, the overall form of the dependence of the HC(O)OC(O)H, HC(O)OH, and CO yields on O_2 partial pressure is well described using $k_{13}/k_{14} = 0.022$ Torr^{-1}.

At this point, it should be noted that the focus of the present investigation was to provide information useful for modeling the atmospheric oxidation of methyl formate. The experiments reported in this section were conducted in the absence of NO_x. In the absence of NO_x, the peroxy radicals derived from methyl formate ($HC(O)OCH_2OO\cdot$ and $\cdot OOC(O)OCH_3$) will undergo self-reaction, cross-reaction, and reaction with HO_2 radicals. There are no kinetic or mechanistic data for such reactions. A detailed interpretation of the product yields observed in the absence of NO_x is not possible at this time and is likely to be of limited relevance to understanding the atmospheric oxidation mechanism of methyl formate. While experiments conducted in the absence of NO_x allow a relatively straightforward determination of k_{13}/k_{14}, they do not provide a good representation of the atmospheric oxidation mechanism of methyl formate in urban air masses. To provide such insight, we conducted the remainder of the experiments described here in the presence of NO_x.

3.4. Calibration of the IR Spectrum of $CH_3OC(O)OONO_2$ at NCAR. Prior to investigating the products of the Cl atom initiated oxidation of methyl formate in the presence of NO_x, a series of experiments was performed to calibrate the IR spectrum of the peroxyacylnitrate $CH_3OC(O)OONO_2$. To obtain a calibrated reference spectrum of $CH_3OC(O)OONO_2$, we subjected mixtures of methyl formate, Cl_2 and NO_2 in air to five photolysis periods of 2 min each. As in the previous studies of Kirchner et al.[21] and Christensen et al.,[22] we observed the appearance of IR absorption features at 797, 928, 1197, 1235, 1304, 1448, 1748, and 1836 cm^{-1}, which are consistent with the formation of a PAN-type molecule (i.e., $CH_3OC(O)OONO_2$). These product features increased linearly with methyl formate loss. In agreement with Christensen et al.[22] (but in contrast to Kirchner et al.[21]), we also observed the formation of the unstable peroxy nitrate $HC(O)OCH_2OONO_2$; the band positions and relative intensities were in good agreement with those reported by Christensen et al.[22] Upon the addition of NO to the system, the $HC(O)OCH_2OONO_2$ decomposed with a lifetime, which was less than 1 min, while the more stable $CH_3OC(O)OONO_2$ persisted in the chamber for more than 30 min. Very little CO_2 (<7%) was detected before the addition of NO, further indicating the thermal stability of the $\cdot C(O)OCH_3$ radical. It seems reasonable to assume that the $CH_3OC(O)OONO_2$ yield is equal to that for H atom abstraction at the formate end of the $CH_3OC(O)H$ molecule. A composite plot of $CH_3OC(O)OONO_2$ absorption at 1836 and 1236 cm^{-1} versus $CH_3OC(O)H$ loss from three experiments using different O_2 partial pressures is shown in Figure 7. Assuming $k_{5a}/(k_{5a} + k_{5b}) = 0.55$ (see section 3.2), the slopes can be used to derive absorption cross sections (base e) of $(1.8 \pm 0.1) \times 10^{-18}$ and $(4.2 \pm 0.2) \times 10^{-18}$ cm^2 molecule^{-1} at 1836 and 1236 cm^{-1}, respectively. While these cross sections are approximately a factor of 2 higher than those normally associated with PAN-type molecules (see Figure 4 in

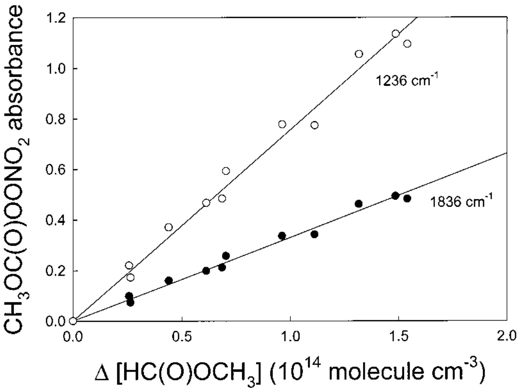

Figure 7. Absorbance of $CH_3OC(O)OONO_2$ at 1236 (open symbols) and 1836 cm^{-1} (filled symbols) vs loss of $HC(O)OCH_3$ following UV irradiation of $HC(O)OCH_3/Cl_2/air/NO_2$ mixtures.

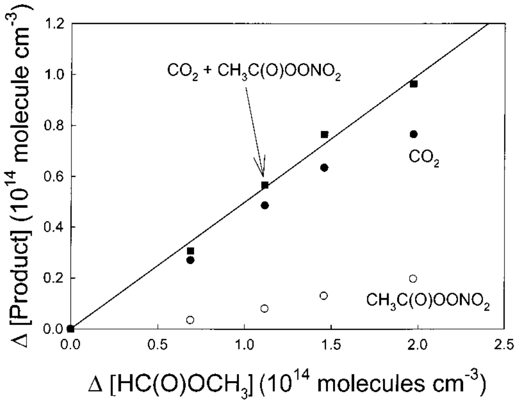

Figure 8. Formation of CO_2 (filled circles), $CH_3OC(O)O_2NO_2$ (open circles), and the sum of CO_2 + $CH_3OC(O)O_2NO_2$ (squares) observed following UV irradiation of $Cl_2/HC(O)OCH_3/NO/N_2/O_2$ mixtures.

Christensen et al.[22]), they are in good agreement with those of the related molecule $CF_3OC(O)O_2NO_2$.[22]

3.5. Products of Cl-Initiated Oxidation of Methyl Formate in the Presence of NO_x. To study the products formed following Cl atom initiated oxidation of methyl formate in the presence of NO_x, we performed experiments using the UV irradiation of $HC(O)OCH_3/Cl_2/NO/N_2/O_2$ mixtures at both NCAR and Wuppertal. Five major carbon containing products were observed, CO, CO_2, HC(O)OH, HC(O)OC(O)H, and $CH_3OC(O)O_2NO_2$, along with traces of CH_3ONO, CH_3ONO_2, and $HC(O)OCH_2O_2NO_2$. Within the experimental uncertainties, the sum of these products accounted for 90−100% of the observed loss of methyl formate. Experiments were conducted using a range of O_2 pressures (2−450 Torr) to examine the O_2 dependence of the various products. For a given O_2 pressure, the amount of CO, HCOOH, and HC(O)OC(O)H was found to vary linearly with the loss of methyl formate. The CO_2 yield was initially around 50% but decreased with increasing reaction time, while the $CH_3OC(O)O_2NO_2$ yield (calculated using the IR cross sections determined in section 3.4) increased with reaction time. The trends in the CO_2 and $CH_3OC(O)O_2NO_2$ yields reflect the competition of NO_2 with NO for $CH_3OC(O)O_2$ radicals with increasing $[NO_2]/[NO]$. However, plots of the sum of CO_2 + $CH_3OC(O)O_2NO_2$ versus the loss of $HC(O)OCH_3$ were always linear. Figure 8 shows a plot of $[CO_2]$, $[CH_3OC(O)O_2NO_2]$, and $[CO_2 + CH_3OC(O)O_2NO_2]$ versus the loss of $HC(O)OCH_3$ for an experiment conducted with 51 Torr of O_2. The line through the $[CO_2 + CH_3OC(O)O_2NO_2]$ data is a least-squares analysis, which gives a yield of 0.51 ± 0.06. In all cases, the sum of CO_2 + $CH_3OC(O)O_2NO_2$ was indistinguishable from 55%, in good agreement with both the CO_2 yield in the NO_x-free experiments (see section 3.3) and our determination of $k_{5a}/(k_{5a}+k_{5b}) = 0.55 \pm 0.07$ (see section 3.2). Thus, we conclude that decomposition is the sole atmospheric fate of $\cdot OC(O)OCH_3$ radicals

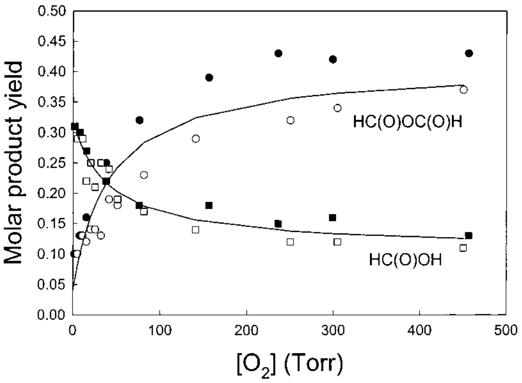

Figure 9. Yields of formic acid anhydride (circles) and HC(O)OH (squares) observed following the UV irradiation of $HC(O)OCH_3/Cl_2/O_2/N_2/NO$ mixtures at 296 K at 700 Torr total pressure of N_2/O_2 diluent vs O_2 partial pressure. Filled symbols represent data taken in Wuppertal, while open symbols are those taken at NCAR.

$$\cdot OC(O)OCH_3 \rightarrow CH_3O\cdot + CO_2 \qquad (16)$$

This finding is consistent with the behavior of the structurally similar acetoxy $(CH_3C(O)O\cdot)$ radical.[5]

Figure 9 shows a plot of the molar HC(O)OH and HC(O)OC(O)H product yields observed in experiments at NCAR (open symbols) and Wuppertal (closed symbols) versus the O_2 partial pressure. There is good agreement in the formic acid yields measured in the two different laboratories, decreasing from about 30% at low O_2 to around 12% at 450 Torr of O_2. Inspection of Figure 9 reveals that there is a difference between the HC(O)OC(O)H yields measured at NCAR and Wuppertal; we ascribe this difference to difficulties associated with the HC(O)OC(O)H analysis. HC(O)OC(O)H has broad unstructured IR features, while HC(O)OH has intense structured IR absorption features. Quantification of the HC(O)OC(O)H is substantially more difficult than that of HC(O)OH.

In all experiments, the $[NO_x]/[O_2]$ concentration ratio was kept below 5×10^{-3} to suppress possible formation of nitrites and nitrates via addition of NO or NO_2 to the alkoxy radicals. The combined yield of HC(O)OC(O)H and HC(O)OH accounts for 50 ± 14% (Wuppertal data) and 41 ± 8% (NCAR data) of the loss of methyl formate. These results are consistent with the branching ratio for Cl atom attack on the methyl group of methyl formate $k_{5b}/(k_{5a} + k_{5b}) = 0.45 \pm 0.07$.

In the presence of NO_x, the peroxy radicals derived from methyl formate $(HC(O)OCH_2OO\cdot$ and $\cdot OOC(O)OCH_3)$ react with NO

$$HC(O)OCH_2OO\cdot + NO \rightarrow HC(O)OCH_2O\cdot + NO_2 \qquad (17a)$$

$$HC(O)OCH_2OO\cdot + NO \rightarrow HC(O)OCH_2ONO_2 \qquad (17b)$$

$$\cdot OOC(O)OCH_3 + NO \rightarrow \cdot OC(O)OCH_3 + NO_2 \qquad (18)$$

Evidence for the formation of the organic nitrate $HC(O)OCH_2ONO_2$ was sought but not found in the IR spectra. Organic nitrates are not lost via heterogeneous reactions or photolysis in the chambers.[23,24] The absence of a substantial yield of $HC(O)OCH_2ONO_2$ is consistent with expectations based upon the behavior of small organic peroxy radicals which typically have low nitrate yields (<5%) in their reaction with NO.[5] Similarly the formation of organic nitrate in reaction 18 is not anticipated.[5] As discussed in section 3.3, the fate of $\cdot OC(O)OCH_3$ radicals is decomposition to give CO_2 and methoxy radicals. The data shown in Figure 9 provide information concerning the relative importance of reaction with O_2 and decomposition via α-ester rearrangement, as fates of $HC(O)OCH_2O\cdot$ radicals formed in reaction 17a

$$HC(O)OCH_2O\cdot + O_2 \rightarrow HO_2 + HC(O)OC(O)H \quad (13)$$

$$HC(O)OCH_2O\cdot + M \rightarrow HCO + HC(O)OH + M \quad (14)$$

The curved line through the HC(O)OC(O)H data in Figure 9 is a fit of expression II to the data using $k_{13}/k_{14} = 0.024$ Torr^{-1}, which is consistent with the result obtained from analysis of product data obtained in the absence of NO_x (see section 3.3). It is interesting to note from Figure 9 that there appears to be a ~10% contribution to the HC(O)OH yield that is independent of the O_2 concentration. The most likely explanation for this observation is that reaction 17a produces a significant yield of excited alkoxy radicals, denoted herein as $HC(O)OCH_2O\cdot^*$, which decompose promptly (i.e., on a time scale that is too short for reaction 13 to compete) to give HC(O)OH. Assuming that reaction 17a leads to the formation of a significant fraction of excited alkoxy radicals $HC(O)OCH_2O\cdot^*$ that possess internal energy exceeding that necessary to overcome the barrier for α-ester rearrangement, the mechanism can be described as follows:

$$HC(O)OCH_2OO\cdot + NO \rightarrow HC(O)OCH_2O\cdot^* + NO_2 \quad (19)$$

$$HC(O)OCH_2O\cdot^* \rightarrow HC(O)OH + HCO\cdot \quad (20)$$

$$HC(O)OCH_2O\cdot^* + M \rightarrow HC(O)OCH_2O\cdot + M^* \quad (21)$$

$$HC(O)OCH_2O\cdot + O_2 \rightarrow HO_2 + HC(O)OC(O)H \quad (13)$$

$$HC(O)OCH_2O\cdot + M \rightarrow HCO + HC(O)OH + M \quad (14)$$

Some fraction of the excited alkoxy radicals undergo prompt decomposition via reaction 20; the remainder will lose their energy through collision with a third body M via reaction 21. Similar chemical activation effects have been reported for the related alkoxy radical formed in the atmospheric oxidation of methyl acetate ($CH_3C(O)OCH_2O\cdot$)[17] and for a variety of other alkoxy radicals (e.g., $CF_3CFHO\cdot$,[25] $HOCH_2CH_2O\cdot$,[26] and $CH_2ClO\cdot$[27]). The yield of HC(O)OH can be expressed as

$$Y(HC(O)OH) = Y(RO\cdot)\left(\frac{1}{\frac{k_{13}}{k_{14}}[O_2] + 1}\right) + Y^* \quad (IV)$$

where $Y(RO\cdot)$ is the fraction of the alkoxy radicals that becomes thermalized and Y^* is the yield of the alkoxy radicals which undergo prompt α-ester rearrangement to give HC(O)OH. A nonlinear least-squares fit of eq IV to the HC(O)OH data in Figure 9 gives $k_{13}/k_{14} = 0.024 \pm 0.004$ Torr^{-1}, $Y(RO\cdot) = 0.20 \pm 0.04$, and $Y^* = 0.12 \pm 0.03$. The fraction of alkoxy radicals which undergo prompt α-ester rearrangement, $Y^* = 0.12 \pm 0.03$, is similar to that measured recently for the analogous alkoxy radical derived from methyl acetate system ($Y^* = 0.20 \pm 0.08$[17]).

Data obtained in sections 3.3 through 3.5 can be used to estimate kinetic and thermodynamic properties for the α-ester rearrangement, reaction 14. With $k_{13}/k_{14} = 0.024$ Torr^{-1} and k_{12} estimated to be 10^{-14} cm^3 molecules^{-1} s^{-1} (by analogy to other alkoxy radical reactions with O_2 [10]), $k_{14} \approx 1.5 \times 10^4$ s^{-1} at 298 K and atmospheric pressure. This rearrangement rate is about 5 times slower than that of the $CH_3C(O)OCH_2O\cdot$ radical derived from methyl acetate, assuming similar O_2 reaction rate coefficients for the two radicals. Finally, the existence of a chemical activation effect in the chemistry of the $HC(O)OCH_2O\cdot$ radical implies that the barrier for reaction 14 is not high, probably no more than 12 kcal/mol.[26]

4. Conclusions

The atmospheric oxidation of methyl formate is initiated by reaction with OH radicals, which gives both $\cdot C(O)OCH_3$ and $HC(O)OCH_2\cdot$ radicals.[28,29] To understand the atmospheric oxidation mechanism of methyl formate, the atmospheric fate of $\cdot C(O)OCH_3$ and $HC(O)OCH_2\cdot$ radicals need to be studied.

A large body of self-consistent data from three laboratories is presented concerning the Cl atom initiated oxidation of methyl formate. Reaction of Cl atoms with methyl formate is found to proceed 45 ± 7% via attack at the methyl group (to give $HC(O)OCH_2\cdot$ radicals) and 55 ± 7% via attack at the formate group (to give $\cdot C(O)OCH_3$ radicals). This result is in contrast to both the structure–activity relationship derived by Notario et al.[13] and the theoretical work of Good et al.,[12] who predicted zero and >70% reactivity at the H–C(O) group, respectively. The sole atmospheric fate of $HC(O)OCH_2\cdot$ and $\cdot C(O)OCH_3$ radicals is addition of O_2 to give the corresponding peroxy radicals ($HC(O)OCH_2OO\cdot$ and $\cdot OOC(O)OCH_3$). The peroxy radicals react with NO to give alkoxy radicals ($HC(O)OCH_2O\cdot$ and $\cdot OC(O)OCH_3$). The atmospheric fate of $\cdot OC(O)OCH_3$ radicals is decomposition to give $CH_3O\cdot$ and CO_2. There are two competing atmospheric loss mechanisms for $HC(O)OCH_2O\cdot$ radicals: reaction with O_2 to give HC(O)OC(O)H and α-ester rearrangement to give HC(O)OH and $HCO\cdot$ radicals. α-Ester rearrangement is more important when $HC(O)OCH_2O\cdot$ radicals were produced via the $HC(O)OCH_2OO\cdot$ + NO reaction than when they were produced via the self-reaction of peroxy radicals. In 1 atm of air ($[O_2] = 160$ Torr) containing NO at 296 K, it can be calculated that 33 ± 6% of the $HC(O)OCH_2O\cdot$ radicals undergo α-ester rearrangement, while 67 ± 12% react with O_2. The value of k_{13}/k_{14} derived here is 5 times smaller than the corresponding value for methyl acetate, suggesting that the α-ester rearrangement is considerably slower in the present case.

Acknowledgment. T.J.W. thanks the Alexander von Humboldt (AvH) Stiftung for an AvH Fellowship. The National Center for Atmospheric Research is operated by the University Corporation for Atmospheric Research under the sponsorship of the National Science Foundation. Financial support by the European Commission and the Bundesministerium für Bildung und Forschung (BMBF) for the work performed at the Bergische Universität GH Wuppertal is gratefully acknowledged.

References and Notes

(1) Japar, S. M.; Wallington, T. J.; Richert, J. F. O.; Ball, J. C. *Int. J. Chem. Kinet.* **1990**, *22*, 1257.

(2) Smith, D. F.; Kleindienst, T. E.; Hudgens, E. E.; McIver, C. D.; Bufalini, J. J. *Int. J. Chem. Kinet*. **1991**, *23*, 97.

(3) Tuazon, E. C.; Carter, W. P. L.; Aschmann, S. M.; Atkinson, R. *Int. J. Chem. Kinet*. **1991**, *23*, 1003.

(4) Wallington, T. J.; Japar, S. M. *Environ. Sci. Technol.* **1991**, *25*, 410.

(5) Lightfoot, P. D.; Cox, R. A.; Crowley, J. N.; Destriau, M.; Hayman, G. D.; Jenkin, M. E.; Moortgat, G. K.; Zabel, F. *Atmos. Environ.* **1992**, *26*, 1805.

(6) Tyndall, G. S.; Cox, R. A.; Granier, C.; Lesclaux, R.; Moortgat, G. K.; Pilling, M. J.; Ravishankara, A. R.; Wallington, T. J. *J. Geophys. Res.*, in press.

(7) Wallington, T. J.; Japar, S. M. *J. Atmos. Chem.* **1989**, *9*, 399.

(8) Barnes, I.; Becker, K. H.; Zhu, T. *J. Atmos. Chem*. **1993**, *17*, 353.

(9) Shetter, R. E.; Davidson, J. A.; Cantrell, C. A.; Calvert, J. G. *Rev. Sci. Instrum*. **1987**, *58*, 1427.

(10) Atkinson, R.; Baulch, D. L.; Cox, R. A.; Hampson, R. F.; Kerr, J. A.; Rossi, M. J.; Troe, J. *J. Phys. Chem. Ref. Data* **1997**, *26*, 521.

(11) Wallington, T. J.; Hurley, M. D.; Ball, J. C.; Jenkin, M. *Chem. Phys. Lett*. **1993**, *211*, 41.

(12) Good, D. A.; Hanson, J.; Kamoboures, M.; Santiono, R.; Francisco, J. S. *J. Phys. Chem. A* **2000**, *104*, 1505.

(13) Notario, A.; Le Bras, G.; Mellouki, A. *J. Phys. Chem. A* **1998**, *102*, 3112.

(14) Meagher, R. J.; McIntosh, M. E.; Hurley, M. D.; Wallington, T. J. *Int. J. Chem. Kinet*. **1997**, *29*, 619.

(15) Bilde, M.; Møgelberg, T. E.; Sehested, J.; Nielsen, O. J.; Wallington, T. J.; Hurley, M. D.; Japar, S. M.; Dill, M.; Orkin, V. L.; Buckley, T. J.; Huie, R. E.; Kurylo, M. J. *J. Phys. Chem. A* **1997**, *101*, 3514.

(16) Tuazon, E. C.; Aschmann, S. M.; Atkinson, R.; Carter, W. P. L. *J. Phys. Chem. A* **1998**, *102*, 2316.

(17) Christensen, L. K.; Ball, J. C.; Wallington, T. J. *J. Phys. Chem. A* **2000**, *104*, 345.

(18) Cavalli, F.; Barnes, I.; Becker, K. H.; Wallington, T. J. *J. Phys. Chem. A* **2000**, *104*, 11310.

(19) Maurer, T.; Hass, H.; Barnes, I.; Becker, K. H. *J. Phys. Chem. A* **1999**, *103*, 5032.

(20) Stein, T. N. N.; Christensen, L. K.; Platz, J.; Sehested, J.; Nielsen, O. J.; Wallington, T. J. *J. Phys. Chem. A* **1999**, *103*, 5705.

(21) Kirchner, F.; Thüner, L. P.; Barnes, I.; Becker, K. H.; Donner, B.; Zabel, F. *Environ. Sci. Technol.* **1997**, *31*, 1801.

(22) Christensen, L. K.; Wallington, T. J.; Guschin, A.; Hurley, M. D. *J. Phys. Chem. A* **1999**, *103*, 4202.

(23) Orlando, J. J.; Iraci, L. T.; Tyndall, G. S. *J. Phys. Chem. A* **2000**, *104*, 5072.

(24) Nozière, B.; Barnes, I.; Becker, K. H. *J. Geophys. Res*. **1999**, *104*, 23645.

(25) Wallington, T. J.; Hurley, M. D.; Fracheboud, J. M.; Orlando, J. J.; Tyndall, G. S.; Sehested, J.; Møgelberg, T. E.; Nielsen, O. J. *J. Phys. Chem*. **1996**, *100*, 18116.

(26) Orlando, J. J.; Tyndall, G. S.; Bilde, M.; Ferronato, C.; Wallington, T. J.; Vereecken, L.; Peeters, J. *J. Phys. Chem. A* **1998**, *102*, 8116.

(27) Bilde, M.; Orlando, J. J.; Tyndall, G. S.; Wallington, T. J.; Hurley, M. D.; Kaiser, E. W. *J. Phys. Chem. A* **1999**, *103*, 3963.

(28) LeCalvé, S.; Le Bras, G.; Mellouki, A. *J. Phys. Chem. A* **1997**, *101*, 5489.

(29) Good, D. A.; Hanson, J.; Francisco, J. S.; Li, Z.; Jeong, G.-R. *J. Phys. Chem. A* **1999**, *103*, 10893.